tecture do incorporate such machinery and thus might form the basis for learning mechanisms that could account for our data [J. E. Hummel and K. J. Holyoak, *Psychol. Rev.* **104**, 427 (1997)]. Our goal is not to deny the importance of neural networks but rather to try to characterize what properties the right sort of neural network architecture must have.

25. Supported in part by an Amherst College Faculty Research Grant to P.M.V. We thank L. Bonatti, M. Brent, S. Carey, J. Dalalakis, P. Gordon, B. Partee, V. Valian, and Z. Zvolenszky for helpful discussion, and P. Marcus and F. Scherer for their assistance in construction of the test apparatus. We also thank Bell Labs for making available to the public the speech synthesizer that we used to create our stimuli. Some subjects in experiment 1 were tested at Amherst College; all other subjects were tested at New York University. The parents of all participants gave informed consent.

11 September 1998; accepted 16 November 1998

Assembly and Analysis of Conical Models for the HIV-1 Core

Barbie K. Ganser,* Su Li,* Victor Y. Klishko, John T. Finch, Wesley I. Sundquist†

The genome of the human immunodeficiency virus (HIV) is packaged within an unusual conical core particle located at the center of the infectious virion. The core is composed of a complex of the NC (nucleocapsid) protein and genomic RNA, surrounded by a shell of the CA (capsid) protein. A method was developed for assembling cones in vitro using pure recombinant HIV-1 CA-NC fusion proteins and RNA templates. These synthetic cores are capped at both ends and appear similar in size and morphology to authentic viral cores. It is proposed that both viral and synthetic cores are organized on conical hexagonal lattices, which by Euler's theorem requires quantization of their cone angles. Electron microscopic analyses revealed that the cone angles of synthetic cores were indeed quantized into the five allowed angles. The viral core and most synthetic cones exhibited cone angles of approximately 19 degrees (the narrowest of the allowed angles). These observations suggest that the core of HIV is organized on the principles of a fullerene cone, in analogy to structures recently observed for elemental carbon.

HIV-1 assembly is initially driven by polymerization of the Gag polyprotein, which forms a spherical shell associated with the inner membrane of the budding particle. The three major regions of Gag all perform essential roles in viral assembly: the NH_2-terminal MA (matrix) region binds the membrane, the central CA (capsid) region mediates important Gag-Gag interactions, and the COOH-terminal NC (nucleocapsid) region packages the viral RNA genome [reviewed in (*1, 2*)]. As the particle assembles, the viral protease cleaves Gag, producing discrete MA, CA, and NC proteins, which subsequently rearrange to form the mature, infectious viral particle. During maturation, MA remains associated with the inner viral membrane, while CA and NC condense about the viral RNA to form an unusual conical structure at the center of the virus (the "core"). The interior of the core is composed of an RNA/NC copolymer, and is surrounded by an outer shell composed of ~1500 copies of CA. The conical core appears to be essential, because Gag mutations that disrupt proper core formation invariably inhibit viral infectivity (*3*). The core probably organizes the viral RNA genome (and its associated enzymes) for uncoating and replication in the new host cell, although these processes are not yet well understood.

Our initial goal was to develop a model system for studying viral core structure and assembly in vitro. The assembly properties of pure recombinant HIV-1 Gag protein fragments have been investigated in several laboratories (*4–7*). Pioneering work by Campbell and Vogt demonstrated that fragments of HIV-1 and Rous sarcoma virus (RSV) Gag proteins that encompass the CA and NC domains can assemble into long hollow cylinders in the presence of RNA (*5*). Building on this, we screened for conditions that would support the assembly of conical (rather than cylindrical) structures. Initially, we employed an HIV-1 RNA template that spanned sites required for genomic RNA packaging (Ψ) and dimerization (DLS), because some models for the viral core have suggested that the genomic RNA dimer dictates the cone morphology (*8*). The protein construct included both the CA and NC domains of HIV-1 Gag, because viral core morphology can be disrupted by mutations in either of these domains, or in the short spacer peptide that connects them (*3*). Finally, solution assembly conditions were varied, because cylinder formation is sensitive to protein and RNA concentrations, salt, and pH (*4–7*). Cone formation was assayed by transmission electron microscopy (TEM) of negatively stained samples.

A mixture of cones (Fig. 1A, arrows) and cylinders formed spontaneously upon incubation of a pure recombinant CA-NC fusion protein with a purified 1400-nucleotide (nt) HIV-1 RNA template in 500 mM NaCl (pH 8.0) (*9*). Cone:cylinder ratios as high as ~2:3 were observed under these optimized conditions. Cones also formed under physiological conditions [that is, 150 mM NaCl (pH 7.2)], albeit at reduced efficiencies. The synthetic cones were capped at both ends, and many appeared strikingly similar to authentic HIV-1 cores (Fig. 1B). Cones formed in vitro varied between 100 and 300 nm in length. Viral cores are typically ~100 nm long (*8, 10*); however, this can also vary considerably because HIV-1 virions range between ~120 to 260 nm in diameter (*11*). These similarities

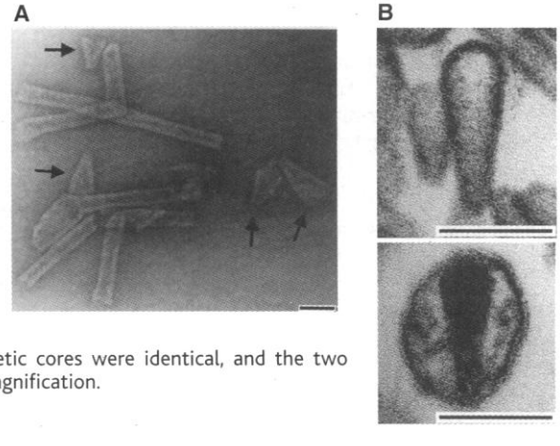

Fig. 1. CA-NC/RNA complexes spontaneously assemble into cones in vitro. (**A**) TEM image of a representative field of negatively stained particles formed by the CA-NC protein on a 1400-nt HIV-1 RNA template. Conical structures are denoted by arrows. Scale bars in Figs. 1, 2, and 4 are 100 nm. (**B**) Selected thin-sectioned TEM images of an authentic HIV-1 virion grown in culture (bottom) and a synthetic CA-NC/RNA cone assembled in vitro (top). Electron microscope preparations of virions and synthetic cores were identical, and the two objects are shown at the same magnification.

B. K. Ganser, S. Li, V. Y. Klishko, W. I. Sundquist, Department of Biochemistry, University of Utah, Salt Lake City, UT 84132, USA. J. T. Finch, Structural Studies Division, UK. Medical Research Council Laboratory of Molecular Biology, Hills Road, Cambridge, CB2 2QH, UK.

*These authors contributed equally to this work.
†To whom correspondence should be addressed. E-mail: wes.sundquist@hsc.utah.edu

suggest that the synthetic cores are accurate structural models for the viral core.

To test whether specific HIV-1 RNA sequences or structures were essential for core formation, we also carried out assembly reactions using noncognate RNA templates (*12*). The 6400-nt RNA from tobacco mosaic virus (TMV) also supported cone formation (Fig. 2A), as did a 1400-nt fragment from the *Bacillus stearothermophilus* 16*S* ribosomal RNA (*13*). Although the efficiency of cone assembly varied considerably in different reactions, these variations did not correlate with the RNA template used. Thus, our experiments seem to rule out models in which specific viral RNA sequences or structures (for example, the DIS structure) account for the asymmetry of the cone (*8*). We then examined assembly of the CA-NC protein in the absence of RNA to determine whether RNA was required at all for cone formation. The CA-NC protein alone could form cones (and cylinders), but only under very high ionic strength conditions (for example, 1 M NaCl) (Fig. 2B) (*12*). Therefore, RNA promotes CA-NC assembly, possibly by concentrating the CA-NC protein or by neutralizing charge, or both, but the polynucleotide chain itself does not play an indispensable structural role. Overall, our experiments demonstrate that the ability to form conical cores is an intrinsic property of the HIV-1 CA-NC complex, and it does not absolutely require an RNA template, the presence of any additional viral or cellular factors, or prior formation of an immature virion.

Although asymmetric, the synthetic cores often appeared highly regular, suggesting that they might be constructed from a regular underlying lattice. Our models for the lattice of the viral core were guided by the recent discovery that elemental carbon can also form cones of varying angles that are capped by different subsurfaces of buckminsterfullerene (*14, 15*). These carbon cones are composed of helices of hexamers arrayed on conical hexagonal lattices (derived from plane group symmetry *p*6) and are closed by pentameric "defects" at the narrow and wide ends of the cone (Fig. 3). From Euler's theorem, the cone angles (θ) of a conical hexagonal lattice will be quantized into the five allowed angles (Fig. 3, A and B) defined by Eq. 1:

$$\sin(\theta/2) = 1 - (P/6) \qquad (1)$$

Fullerene cones can be capped by the introduction of pentameric "defects" at the narrow and wide ends of the cone, with each pentamer surrounded by five hexamers (as in buckminsterfullerene). The cone angle determines the number of pentamers (P) required to close the narrow end of the cone (where P is an integer between 0 and 6), with narrower cone angles closed by larger numbers of pentamers.

We propose that HIV-1 cores form cones using the same symmetry principles as carbon. In our model, the viral core assembles on a curved *p*6 lattice, with five pentameric defects arrayed in a $P = 5$ configuration at the narrow end (Fig. 3, C and D). Because a total of 12 pentameric defects are required to create a closed object from a hexagonal lattice, the wide end of the cone will be capped with an additional seven pentameric defects. The precise distribution of the pentamers and their distribution will determine the shapes of the caps. The driving force for closing the conical lattice could be saturation of all possible CA interfaces, as has also been observed for carbon cones (*14*).

To the best of our knowledge, accurate measurements of HIV-1 core angles have not been reported, but crude three-dimensional (3D) reconstructions of the core appear to us to be consistent with the narrow (19.2°) cone angle predicted for a $P = 5,7$ cone (*8, 16*). Cryo–electron microscopic images of our synthetic cores in vitreous ice similarly suggested the presence of $P = 5,7$ cones (*17*). These analyses were complicated, however, because the synthetic cores could adopt a range of different orientations, and tilting a cone with respect to the horizontal widens the observed cone angle. Thus, the minimum observed cone angle for frozen cores was ~19°, but a distribution of larger cone angles was also observed (*18*).

To test whether the cone angles of synthetic cores were quantized according to Eq.

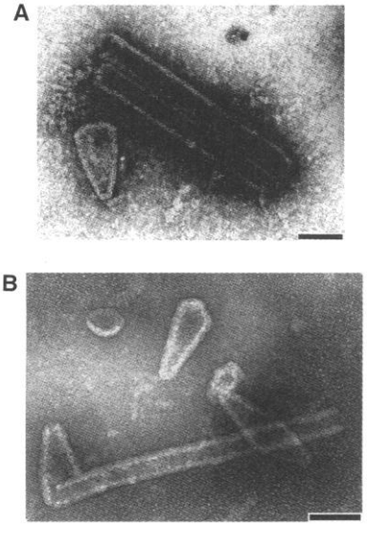

Fig. 2. (**A**) Particles formed by CA-NC protein on a 6400-nt TMV RNA template. (**B**) Particles formed by the CA-NC protein in high salt concentration (1M NaCl) in the absence of RNA.

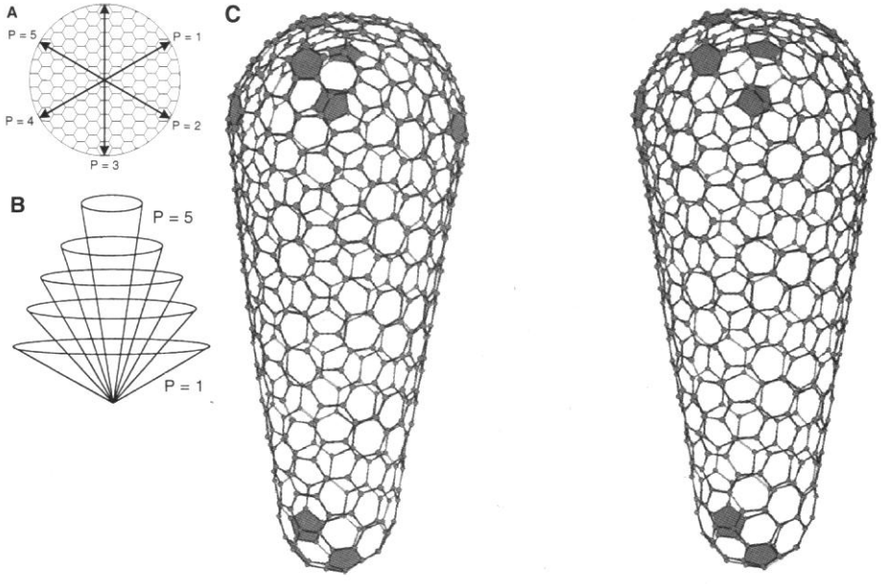

Fig. 3. (**A**) Quantization of the angles of cones derived from conical hexagonal (*p*6) lattices. A cone can be created by cutting along the vertical line at the top of the circle, making a second cut along another lattice line, removing the intervening slice, and resealing the two interfaces (with or without helical skew). Note, however, that if the second cut is made off a lattice line, the cone cannot be resealed without disruption of the hexagonal lattice. (**B**) The five allowable angles resulting from the conical constructs described in (A). Allowable cone angles are 112.9° ($P = 1$ cap), 83.6° ($P = 2$), 60° ($P = 3$), 38.9° ($P = 4$), and 19.2° ($P = 5$). (**C**) Stereoview of a capped 19.2° fullerene cone composed of 252 hexagons and 12 pentagons. Pentagons within the narrow ($P = 5$) and wide ($P = 7$) caps are shaded. Note that alternative arrangements of the pentagons will alter the shapes of the caps. (**D**) End-on view of a $P = 5$ cap configuration. The five pentagons at the apex of the cone are shaded. Figure parts (A) through (D) were adapted from (*14*) and drawn using Chem3D Ultra (Cambridge Software).

1, oriented samples were prepared for TEM under dehydrating conditions, thereby flattening the cores onto an underlying Formvar/carbon grid (*19*). The measured angle (ϕ) for a cone flattened onto a horizontal surface is related to the original cone angle (θ) by Eq. 2.

$$\phi = 180° \sin(\theta/2) \quad (2)$$

Hence, if our model is correct, ϕ angles for the flattened synthetic cores should be quantized in increments of 30° (that is, a $P = 5$ configuration with a cone angle $\theta = 19.2°$ will flatten to give an observed cone angle $\phi = 30°$; the other allowable cone angles will be 60°, 90°, 120°, and 150°). Measured ϕ angles did, in fact, fall into five groups that were integral multiples of 30° (Fig. 4). Narrow ($P = 5,7$) cones predominated, with approximately 90% of all of the cones examined exhibiting a ~30° cone angle. This prevalence may reflect preferential nucleation of the narrow conical lattice or the reduced strain of the $P = 5$ cap configuration versus $P = 2$–4 configurations (*14*). Although

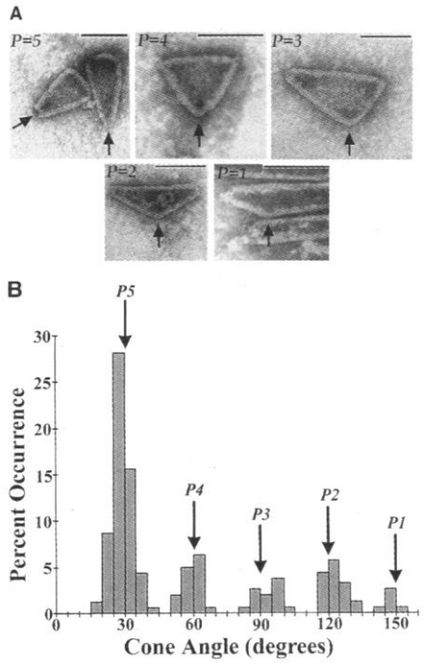

Fig. 4. Cone angle distribution in negatively stained TEM images of synthetic cores. **(A)** Examples of synthetic cones with putative P = 1–5 caps (arrows). **(B)** Histogram showing the relative occurrence of different cone angles. Theoretical values for (flattened) cones with P = 1–5 cap configurations are denoted by arrows. Randomly selected, discrete cones or conical disclinations were measured from photographic images of fields of negatively stained CA-NC/TMV RNA particles (n = 160). Cones exhibiting obvious curvature or obscured by other particles were excluded from the measurements. Experimental cone angles and standard deviations for the five different groups were: 29 ± 4 (P = 5 cap), 59 ± 4 (P = 4), 94 ± 6 (P = 3), 123 ± 5 (P = 2), 148 ± 2 (P = 1).

rarer than the $P = 5,7$ cones, examples of all other predicted cone angles were also observed. The fact that the CA-NC/RNA complexes formed five (and only five) discrete cone angles, as well as flat sheets (that is, $P = 0$) and cylinders (that is, $P = 6$) (*4*), strongly implies that a hexagonal lattice symmetry underlies cone formation.

Our model for the organization of the viral core requires that the CA protein shell (and possibly also the internal NC/RNA complex) adopt a curved *p6* lattice. Lattices containing cages of hexameric rings have been proposed for various protein arrays thought to mimic immature retroviral Gag shells (although the precise arrangements of protein subunits differ between the models) (*20*). More recently, we have performed cryo–electron microscopic image reconstructions of hollow cylinders formed by the mature HIV-1 CA protein (*4*) and have shown that these cylinders are, in fact, composed of CA hexagons arrayed on helical *p6* lattices (*21*). Thus, these reconstructions provide direct experimental evidence that CA can spontaneously assemble into precisely the arrangement required by our model for the viral core.

Although the unusual conical shape of the HIV-1 core is characteristic of lentiviruses, other classes of retroviruses can have cylindrical cores (D-type) or spherical cores that can be centrically (C-type) or acentrically (B-type) positioned within the virion (*22*). Despite this morphological diversity, it is intuitively appealing to believe that these different shapes are created using similar underlying structural principles, particularly as retroviral Gag sequences share primary sequence similarities (*23*). An attractive aspect of our model is that the cores of all retroviruses could be composed of closed hexagonal lattices and differ simply in the spacing of their pentameric defects, thereby creating either spheres, cylinders, or cones.

References and Notes

1. H.-G. Kräusslich, Ed., *Morphogenesis and Maturation of Retroviruses*, vol. 214 of *Current Topics in Microbiology and Immunology* (Springer-Verlag, Berlin, 1996).
2. R. Swanstrom and J. W. Wills, in *Retroviruses*, J. M. Coffin, S. H. Hughes, H. E. Varmus, Eds. (Cold Spring Harbor Laboratory Press, Plainview, NY, 1997), pp. 263–334.
3. T. Dorfman, J. Luban, S. P. Goff, W. A. Haseltine, H. G. Göttlinger, *J. Virol.* **67**, 6159 (1993); T. Dorfman, A. Bukovsky, Å. Öhagen, S. Höglund, H. G. Göttlinger, *ibid.* **68**, 8180 (1994); F. Mammano, Å. Öhagen, S. Höglund, H. G. Göttlinger, *ibid.*, p. 4927; A. S. Reicin *et al.*, *ibid.* **69**, 642 (1995); A. S. Reicin, A. Ohagen, L. Yin, S. Höglund, S. P. Goff, *ibid.* **70**, 8645 (1996); D. T. K. Poon, J. Wu, A. Aldovini, *ibid.*, p. 6607; M. A. Accola, S. Höglund, H. G. Göttlinger, *ibid.* **72**, 2072 (1998); V. Tanchou *et al.*, *ibid.*, p. 4442; U. K. von Schwedler, K. Stray, V. Y. Klishko, W. I. Sundquist, in preparation.
4. L. S. Ehrlich, B. E. Agresta, C. A. Carter, *J. Virol.* **66**, 4874 (1992); I. Groß, H. Hohenberg, H.-G. Kräusslich, *Eur. J. Biochem.* **249**, 592 (1997).
5. S. Campbell and V. M. Vogt, *J. Virol.* **69**, 6487 (1995); *ibid.* **71**, 4425 (1997).
6. U. K. von Schwedler *et al.*, *EMBO J.* **17**, 1555 (1998).
7. I. Groß, H. Hohenberg, C. Huckhagel, H.-G. Kräusslich, *J. Virol.* **72**, 4798 (1998).
8. S. Höglund *et al.*, *AIDS Res. Hum. Retroviruses* **8**, 1 (1992).
9. An expression plasmid for the HIV-1_{NL4-3} CA-NC protein (HIV-1_{NL4-3} Gag amino acids 133–433) was created by polymerase chain reaction amplification of the coding sequence from the plasmid pNL4-3 (obtained from the NIH AIDS Research and Reference Reagent Program) [A. Adachi *et al.*, *J. Virol.* **59**, 284 (1986)]. The amplified DNA was subcloned into the Nde I and Bam HI cloning sites of the pET11a expression vector (Novagene), and the resulting plasmid (WISP96-18) was confirmed by dideoxy sequencing. The CA-NC protein was expressed in freshly transformed BL21(DE3) cells [4 liters of culture, 4-hour induction with 1 mM isopropyl-β-D-thiogalacopyranoside, optical density at 600 nm (OD_{600}) = 0.6]. Cells were harvested by centrifugation, resuspended in 30 ml of 0.5 M NaCl in buffer A [20 mM tris-HCl (pH 7.5), 1 μM $ZnCl_2$, 10 mM 2-mercaptoethanol, 1 tablet protease inhibitor (Boehringer Mannheim)], and lysed by passage through a French Press, then the lysate was sonicated to reduce viscosity (this and all subsequent steps were performed at 4°C). Insoluble cellular debris was removed by centrifugation at 35,000*g* for 30 min. Nucleic acids were stripped from the soluble protein by the addition of 0.11 equivalents (v/v) of 2 M $(NH_4)_2SO_4$, followed by addition of the same volume of 10% polyethylenimine (pH 8.0). The mixture was stirred for 20 min, and the nucleic acid precipitate removed by centrifugation at 29,500*g* for 15 min. The protein was recovered from the supernatant by the addition of 0.35 equivalents saturated $(NH_4)_2SO_4$ solution, stirred for 15 min, and collected by centrifugation at 9820*g*. For chromatography, the protein was redissolved in 30 ml of 0.1 M NaCl in buffer A, dialyzed three times against 1 liter of 50 mM NaCl in buffer A, and clarified by centrifugation and filtration through a 0.2-μm filter. The protein was chromatographed on an SP-Sepharose column (Pharmacia) and eluted at approximately 400 mM NaCl from a linear gradient of 0 to 1 M NaCl in buffer A. Fractions containing the protein were pooled, desalted by dialysis against 3 liters of buffer A, and concentrated under nitrogen by ultrafiltration in an Amicon concentrator. Typical purified yields were ~12 mg/liter of culture. The pure protein was characterized by NH_2-terminal sequencing and mass spectrometry. The initiator methionine was lost during expression, and the NH_2-terminus of CA-NC (PIVQNLQGQM) (*24*) thus corresponded exactly to that of the viral CA protein. The major peak in the mass spectrum of the apoprotein corresponded exactly to the expected mass of CA-NC (MW_{obs} = 33,385 ± 17 daltons, MW_{calc} = 33,385 daltons), although minor species were also observed at masses of 31,343; 32,596; 34,472; 36,101; and 36,841 daltons. CA-NC/RNA cones formed spontaneously upon incubation of the CA-NC protein with RNA for 1 hour at 37°C under the following conditions: 0.3 mM CA-NC, 3 mM RNA (that is, 1 protein molecule/10 nt), 500 mM NaCl, 50 mM tris-HCl (pH 8.0). Cones were also observed at neutral pH and over a range of 100 to 750 mM NaCl. Cone formation was monitored by TEM, either in negatively stained samples deposited directly on Formvar-coated copper grids or in positively stained thin-sectioned samples (*6*). A full survey of the assembly conditions and protein requirements for cone formation will be reported elsewhere.
10. H. R. Gelderblom, E. H. S. Hausmann, M. Özel, G. Pauli, M. A. Koch, *Virology* **156**, 171 (1987).
11. S. D. Fuller, T. Wilk, B. E. Bowen, H.-G. Kräusslich, V. M. Vogt, *Curr. Biol.* **7**, 729 (1997).
12. HIV-1 and ribosomal RNAs were produced by T7 RNA polymerase transcription from linearized DNA templates, purified through a Micro Biospin 6 column (Bio-Rad), and precipitated from ethanol. The transcribed HIV-1 RNA corresponded to the first 1448 nt of the HIV-1_{NL4-3} genome and the ribosomal RNA (control) was a 1441-nt fragment from 16*S* ribosomal RNA of *B. stearothermophilus*. The 6400-nt tobac-

co mosaic viral RNA was obtained by phenol and chloroform extractions of the virus and precipitated from ethanol. CA-NC assembly reactions in the presence of noncognate RNAs were identical to those given in (9). In the absence of RNA, CA-NC cones formed under the following conditions: 300 μM CA-NC, 1 M NaCl, and 50 mM tris-HCl (pH 8.0) at 37°C for 60 min. In the absence of exogenous RNA, neither cones nor cylinders formed at concentrations of 0.5 M NaCl or below. Absorption spectra demonstrated that our CA-NC preparations were not contaminated with *Escherichia coli* RNA (estimated lower detection limit was ~1 base/protein molecule). To control for even lower levels of RNA contamination, we preincubated the CA-NC protein with 0.5 mg/ml ribonuclease A (Type 1-AS, 54 Kunitz U/mg, Sigma) for 1 hour at 4°C, which then formed cones normally.

13. V. Y. Klishko, data not shown.
14. M. Ge and K. Sattler, *Chem. Phys. Lett.* **220**, 192 (1994).
15. A. Krishnan *et al.*, *Nature* **388**, 451 (1997).
16. L. B. Kong *et al.*, *J. Virol.* **72**, 4403 (1998).
17. Assembly mixtures were deposited on holey carbon grids, blotted briefly with filter paper, plunged into liquid ethane, and transferred to liquid nitrogen. Frozen grids were transferred to a Philips 420 TEM equipped with a Gatan cold stage system, and images of particles in vitreous ice were recorded under low dose conditions at 36,000× magnification and ~1.6-μm defocus.
18. J. T. Finch, data not shown.
19. R. A. Crowther, *Proceedings of the Third John Innes Symposium* (1976), pp. 15–25; E. Kellenberger, M. Häner, M. Wurtz, *Ultramicroscopy* **9**, 139 (1982); J. Seymore and D. J. DeRosier, *J. Microsc.* **148**, 195 (1987).
20. M. V. Nermut, C. Grief, S. Hashmi, D. J. Hockley, *AIDS Res. Hum. Retroviruses* **9**, 929 (1993); M. V. Nermut *et al.*, *Virology* **198**, 288 (1994); E. Barklis, J. McDermott, S. Wilkens, S. Fuller, D. Thompson, *J. Biol. Chem.* **273**, 7177 (1998); E. Barklis *et al.*, *EMBO J.* **16**, 1199 (1997); M. Yeager, E. M. Wilson-Kubalek, S. G. Weiner, P. O. Brown, A. Rein, *Proc. Natl. Acad. Sci. U.S.A.* **95**, 7299 (1998).
21. J. T. Finch *et al.*, unpublished observations.
22. V. M. Vogt, in (2), pp. 27–70.
23. M. A. McClure, M. S. Johnson, D.-F. Feng, R. F. Doolittle, *Proc. Natl. Acad. Sci. U.S.A.* **85**, 2469-2473 (1988).
24. Single-letter abbreviations for the amino acid residues are as follows: A, Ala; C, Cys; D, Asp; E, Glu; F, Phe; G, Gly; H, His; I, Ile; K, Lys; L, Leu; M, Met; N, Asn; P, Pro; Q, Gln; R, Arg; S, Ser; T, Thr; V, Val; W, Trp; and Y, Tyr.
25. We thank C. Hill for very helpful discussions on the relationship between viral cores and fullerene cones, D. Hobbs for refining the ChemDraw3D images of cones, G. Stubbs for a gift of tobacco mosiac virus, J. McCutcheon for the plasmid used to prepare ribosomal RNA, and K. Albertine and N. Chandler of the University of Utah Shared Electron Microscopy facility for their support and encouragement. Supported by grants from NIH and from the Huntsman Cancer Institute (to W.I.S.).

29 September 1998; accepted 17 November 1998

The Transcriptional Program in the Response of Human Fibroblasts to Serum

Vishwanath R. Iyer, Michael B. Eisen, Douglas T. Ross, Greg Schuler, Troy Moore, Jeffrey C. F. Lee, Jeffrey M. Trent, Louis M. Staudt, James Hudson Jr., Mark S. Boguski, Deval Lashkari, Dari Shalon, David Botstein, Patrick O. Brown*

The temporal program of gene expression during a model physiological response of human cells, the response of fibroblasts to serum, was explored with a complementary DNA microarray representing about 8600 different human genes. Genes could be clustered into groups on the basis of their temporal patterns of expression in this program. Many features of the transcriptional program appeared to be related to the physiology of wound repair, suggesting that fibroblasts play a larger and richer role in this complex multicellular response than had previously been appreciated.

The response of mammalian fibroblasts to serum has been used as a model for studying growth control and cell cycle progression (*1*). Normal human fibroblasts require growth factors for proliferation in culture; these growth factors are usually provided by fetal bovine serum (FBS). In the absence of growth factors, fibroblasts enter a nondividing state, termed G_0, characterized by low metabolic activity. Addition of FBS or purified growth factors induces proliferation of the fibroblasts; the changes in gene expression that accompany this proliferative response have been the subject of many studies, and the responses of dozens of genes to serum have been characterized.

We took a fresh look at the response of human fibroblasts to serum, using cDNA microarrays representing about 8600 distinct human genes to observe the temporal program of transcription that underlies this response. Primary cultured fibroblasts from human neonatal foreskin were induced to enter a quiescent state by serum deprivation for 48 hours and then stimulated by addition of medium containing 10% FBS (*2*). DNA microarray hybridization was used to measure the temporal changes in mRNA levels of 8613 human genes (*3*) at 12 times, ranging from 15 min to 24 hours after serum stimulation. The cDNA made from purified mRNA from each sample was labeled with the fluorescent dye Cy5 and mixed with a common reference probe consisting of cDNA made from purified mRNA from the quiescent

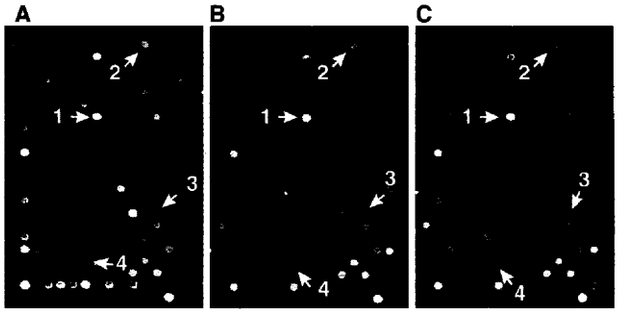

Fig. 1. The same section of the microarray is shown for three independent hybridizations comparing RNA isolated at the 8-hour time point after serum treatment to RNA from serum-deprived cells. Each microarray contained 9996 elements, including 9804 human cDNAs, representing 8613 different genes. mRNA from serum-deprived cells was used to prepare cDNA labeled with Cy3–deoxyuridine triphosphate (dUTP), and mRNA harvested from cells at different times after serum stimulation was used to prepare cDNA labeled with Cy5-dUTP. The two cDNA probes were mixed and simultaneously hybridized to the microarray. The image of the subsequent scan shows genes whose mRNAs are more abundant in the serum-deprived fibroblasts (that is, suppressed by serum treatment) as green spots and genes whose mRNAs are more abundant in the serum-treated fibroblasts as red spots. Yellow spots represent genes whose expression does not vary substantially between the two samples. The arrows indicate the spots representing the following genes: 1, protein disulfide isomerase-related protein P5; 2, IL-8 precursor; 3, EST AA057170; and 4, vascular endothelial growth factor.

V. R. Iyer and D. T. Ross, Department of Biochemistry, Stanford University School of Medicine, Stanford CA 94305, USA. M. B. Eisen and D. Botstein, Department of Genetics, Stanford University School of Medicine, Stanford CA 94305, USA. G. Schuler and M. S. Boguski, National Center for Biotechnology Information, Bethesda MD 20894, USA. T. Moore and J. Hudson Jr., Research Genetics, Huntsville, AL 35801, USA. J. C. F. Lee, D. Lashkari, D. Shalon, Incyte Pharmaceuticals, Fremont, CA 94555, USA. J. M. Trent, Laboratory of Cancer Genetics, National Human Genome Research Institute, National Institutes of Health, Bethesda, MD 20892, USA. L. M. Staudt, Metabolism Branch, Division of Clinical Sciences, National Cancer Institute, Bethesda, MD 20892, USA. P. O. Brown, Department of Biochemistry and Howard Hughes Medical Institute, Stanford University School of Medicine, Stanford CA 94305, USA.

*To whom correspondence should be addressed. E-mail: pbrown@cmgm.stanford.edu